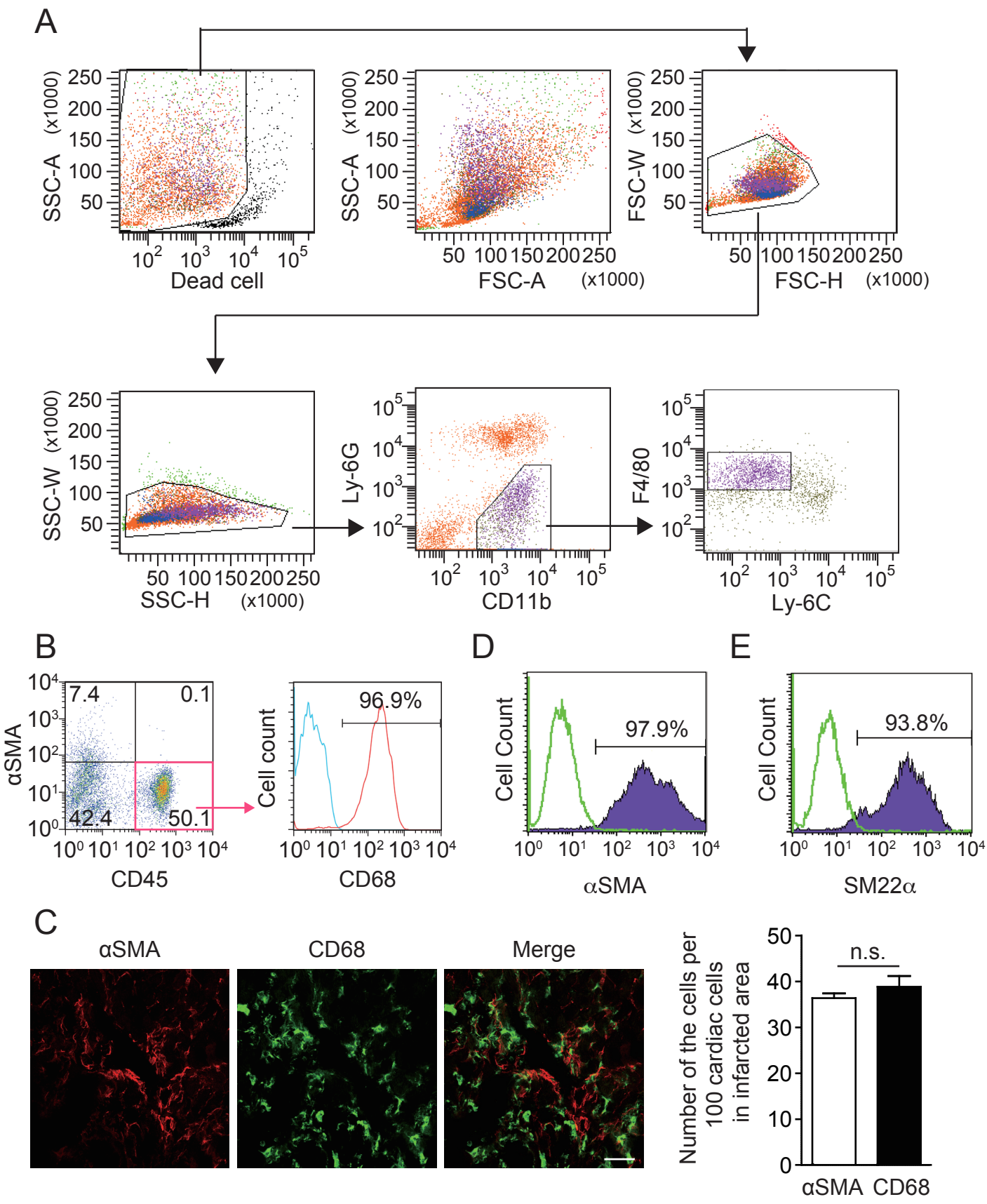

Supplemental Figure 1. Gating strategy for the sorting of cardiac macrophages after MI, and the purity of isolated cardiac myofibroblasts.

(A) Three days after MI, mouse hearts were excised and digested by Dispase II solution. Isolated cells were stained with eFluor 780 viability dye and antibodies against CD11b, Ly-6G, F4/80, and Ly-6C. After the elimination of dead cells and singlet gating, $CD11b^{+}$ $Ly\text{-}6G^{-}$ $F4/80^{high}$ $Ly\text{-}6C^{low}$ cells were sorted as cardiac macrophages by FACSAria III. The collected macrophages were used for the phagocytosis assay ($n = 4$). (B) The cardiac cells collected from infarcted hearts were attached to the plates overnight and were stained with antibodies against CD45, CD68, and αSMA ($n = 4$). (C) Immunohistochemical images of αSMA (red) and CD68 (green) positive cells in the infarcted area of mouse hearts at day 3 after MI ($n = 4$). The number of the cells per 100 caridiac cells in infarcted area is shown in the graph. Scale bar, 50 μm. Error bars represent the mean ± SEM. Comparisons between two groups were assessed with unpaired two tailed Student's *t* test. n.s., not significant. (D and E) The isolated cells as cardiac myofibroblasts were cultured in 10-cm dishes. Three days after isolation, cultured cells were stained with antibodies against αSMA (D) or SM22α (E), and their expression were analyzed by FACSCalibur ($n = 4$ each). Representative FACS profiles were shown.

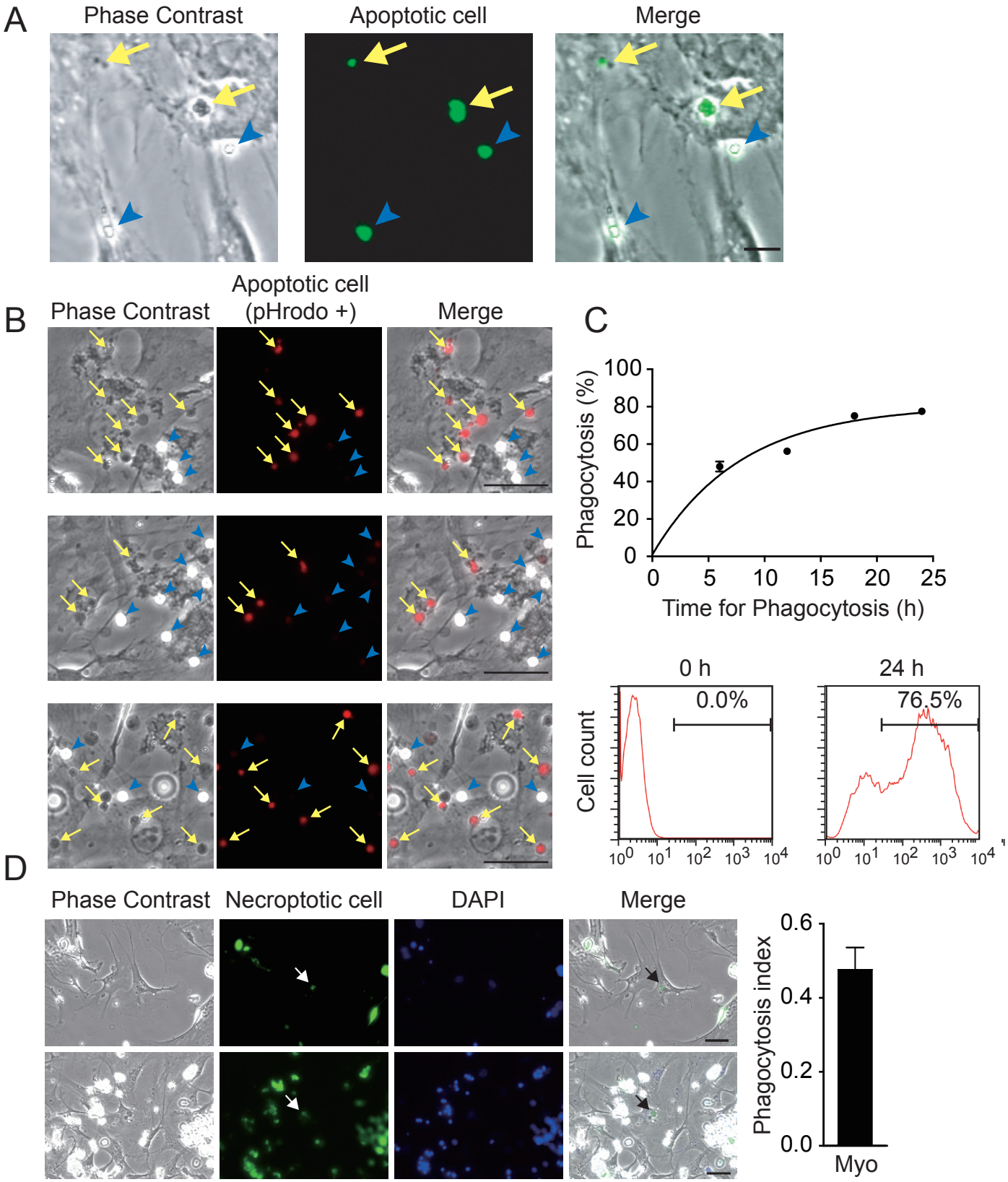

Supplemental Figure 2. *Ex vivo* phagocytosis assay using myofibroblasts and fluorescently labeled apoptotic and necroptotic cells.

(A) Myofibroblasts after the engulfment of fluorescently labeled apoptotic cells were observed under microscopy. The phase-dark apoptotic thymocytes (indicated by yellow arrows) were determined as engulfed apoptotic cells. By contrast, the phase-bright apoptotic thymocytes (indicated by blue arrowheads) were determined as unengulfed (attached) apoptotic cells. Scale bar, 20 μm. (B) pHrodo-labeled thymocytes were incubated with myofibroblasts (n = 6). The engulfed apoptotic thymocytes (indicated by yellow arrows) were pHrodo-positive. In contrast, the unengulfed apoptotic thymocytes (indicated by blue arrowheads) were pHrodo-negative. Scale bar, 20 μm. (C) Cardiac myofibroblasts were co-incubated with CellTrace labeled apoptotic cells for 0, 6, 12, 18, and 24 h. After the incubation, cardiac myofibroblast were harvested and subsequently stained with antibodies for αSMA (n = 3). The uptake of fluorescence was evaluated by flow cytometer. The fitted curve plot was shown. Representative FACS profiles for 0 h and 24 h engulfment were shown. (D) Ex vivo phagocytosis assay of necroptotic cells. Isolated cardiac myofibroblasts were exposed to necroptotic L929 cells (green) (n = 3). The number of engulfed necroptotic cell per cardiac myofibroblast (Myo) was shown. Images were taken at 12–15 randomly selected fields (×40), and over 150 myofibroblasts were evaluated and the phagocytosis index was determined. Representative images taken at the two fields were shown. Arrows indicate engulfed necroptotic cells. Scale bar, 100 μm.

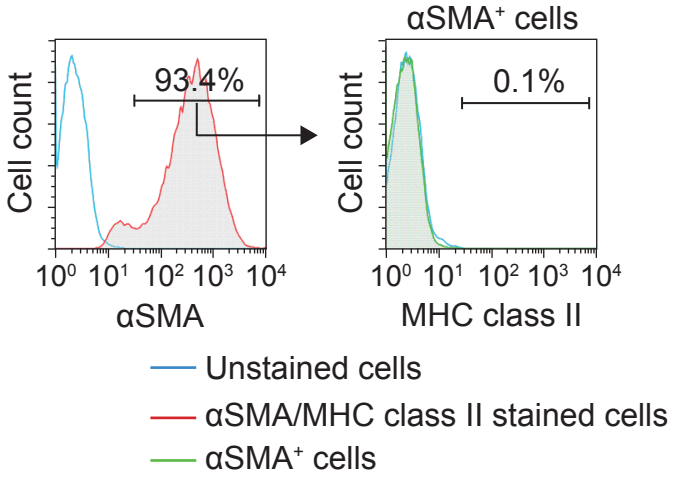

Supplemental Figure 3. αSMA-positive cardiac myofibroblasts do not express MHC class II. Isolated cardiac myofibroblasts were harvested by treatment with accutase and immediately stained with antibodies for αSMA and MHC class II. After gating by αSMA expression, MHC class II expression on α SMA-positive cells was analyzed.

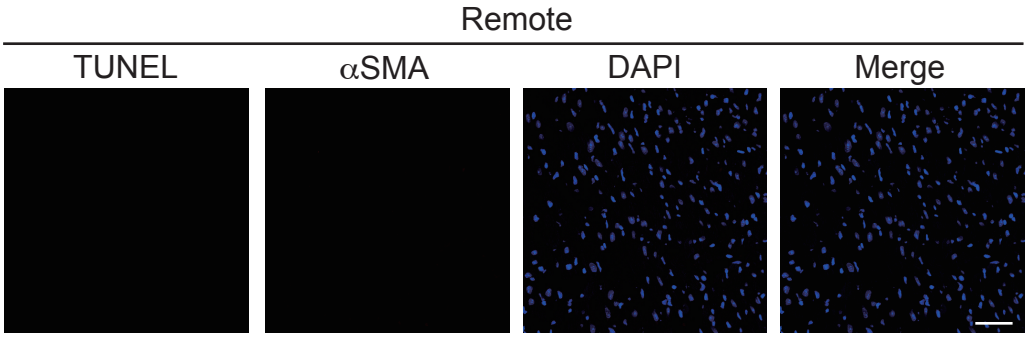

Supplemental Figure 4. Apoptotic cells and myofibroblasts were not detected in remote area of MI-operated mice hearts.
Representative images of remote area of LV sections from WT mice 3 days after MI operation. These sections were double-stained with TUNEL (green) and anti-αSMA antibody (red) (*n* = 4). Scale bar, 50 μm.

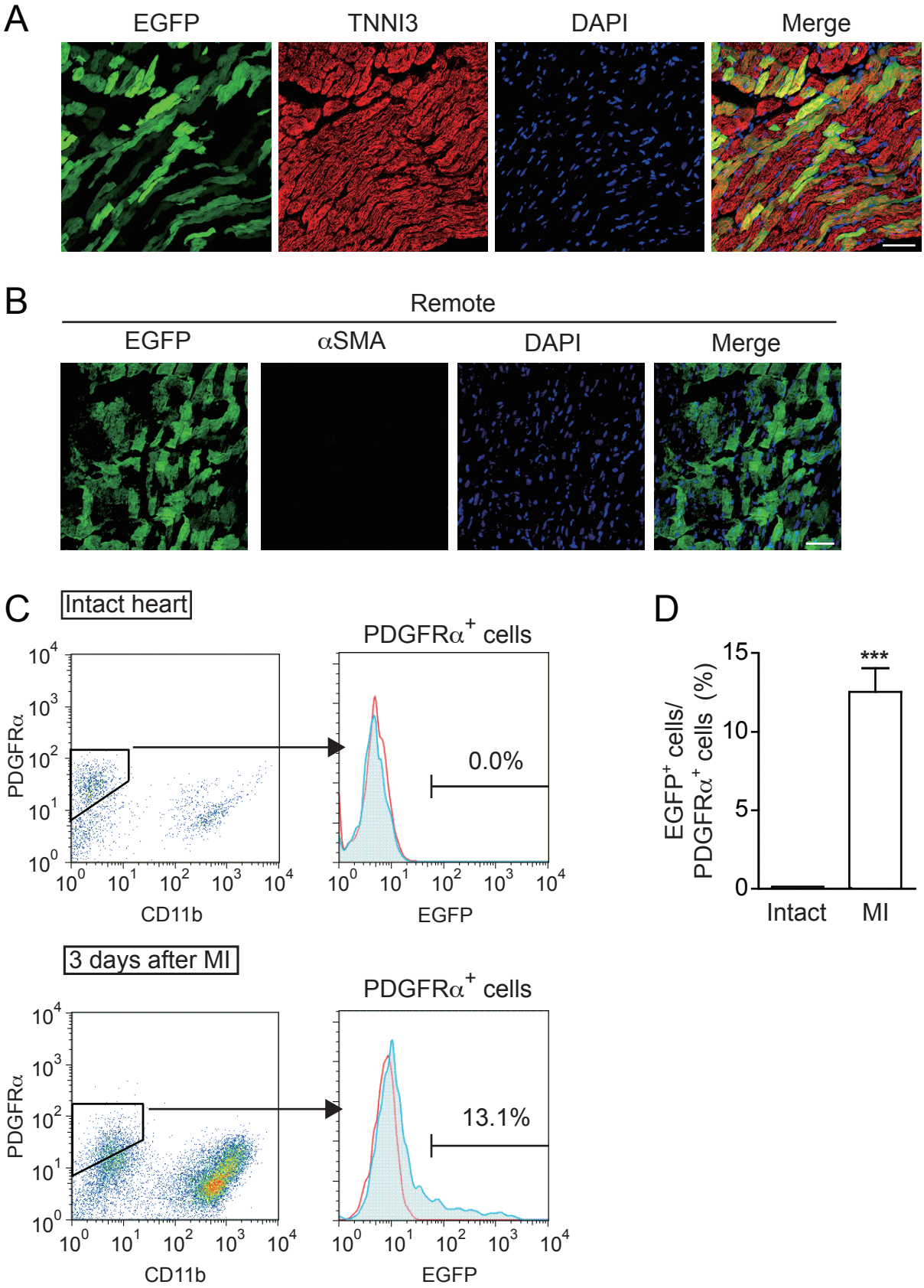

Supplemental Figure 5. EGFP labeling, used for cardiomyocytes, was found in fibroblasts in mouse hearts after MI, but not in intact mouse hearts.

(A) Heart sections from mice injected with AAV9 carrying EGFP under the control of cTnT promoter were stained with antibody against anti-troponin I type 3 (TNNI3, red) (n = 4). Scale bar, 50 μm. (B) Representative images of remote area of LV sections from WT mice with EGFP-labeled cardiomyocytes at 3 days after MI. These sections were stained with anti-GFP (green) and anti-αSMA antibodies (red) (n = 4). Scale bar, 50 μm. (C) The hearts of mice injected with AAV9 carrying EGFP under the control of cTnT promoter were excised and digested by collagenase II and elastase cocktail. Isolated cells from intact hearts (n = 4) and MI-operated hearts (n = 4) were stained with antibodies against PDGFRα and CD11b. After gating viable and singlet cells, PDGFRα$^+$ cardiac fibroblasts (CD11b negative) were further gated, and EGFP expression in cardiac fibroblasts was analyzed. The representative staining profiles of isolated cells are shown. (D) The graph shows the percentage of PDGFRα$^+$ cardiac fibroblasts isolated from intact hearts or MI-operated hearts which contained EGFP. Comparisons between two groups were assessed with unpaired two tailed Student's t test. *** $P < 0.001$.

A

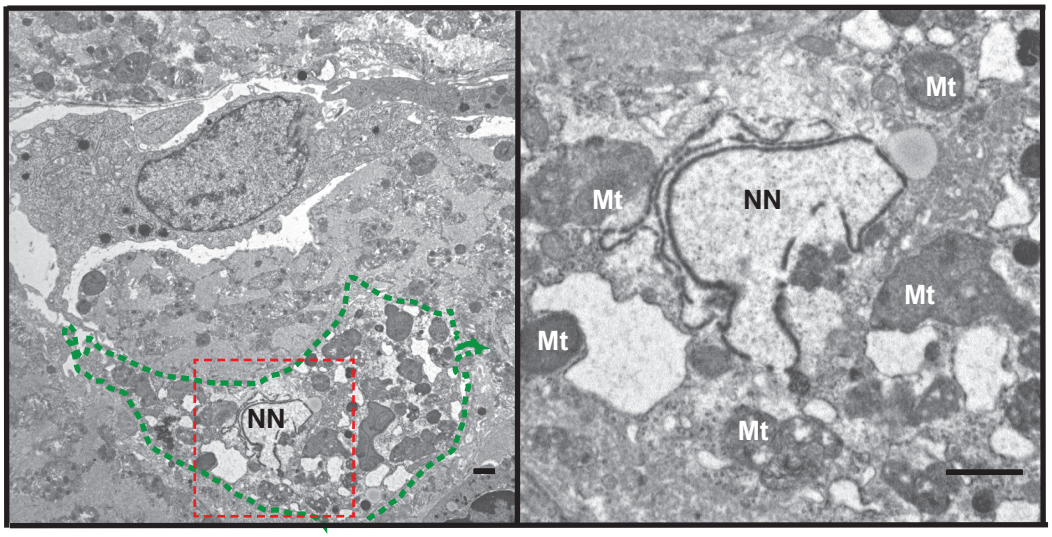

B

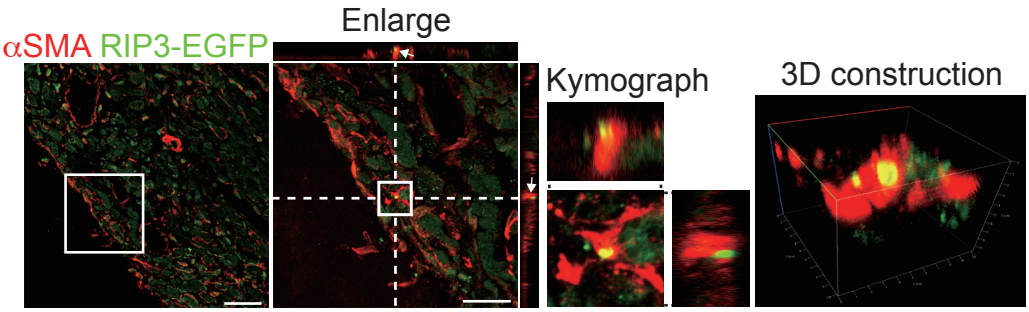

Supplemental Figure 6. Transmission electron micrographs of a necrotic cardiomyocyte and engulfment of a necroptotic cell by a cardiac myofibroblast.
(A) Representative images of a necrotic cardiomyocyte on a section of infarcted mouse heart 3 days after MI. A cardiomyocyte was identified by abundant mitochondria. In the cardiomyocytes (green dotted line), an extensively degraded nucelus, which is a characteristics of necrotic nucleus, was obsereved. The area surrounded by red dotted box was enlarged in the right panel. NN: Necrotic Nucleus, Mt: Mitochondria. Scale bar, 1μm. (B) Representative infarcted LV sections from WT mice with RIP3-EGFP-labeled cardiomyocytes were stained with anti-αSMA antibody (Red) (*n* = 4). Kymographs along the white dashed line in the merged image were shown in the upper and right side of the image. The area indicated by a white square on the merged image was enlarged. White arrows indicate myofibroblasts containing a necroptotic cardiomyocyte. Scale bar, 50 μm (Merge) and 20 μm (Enlarge).

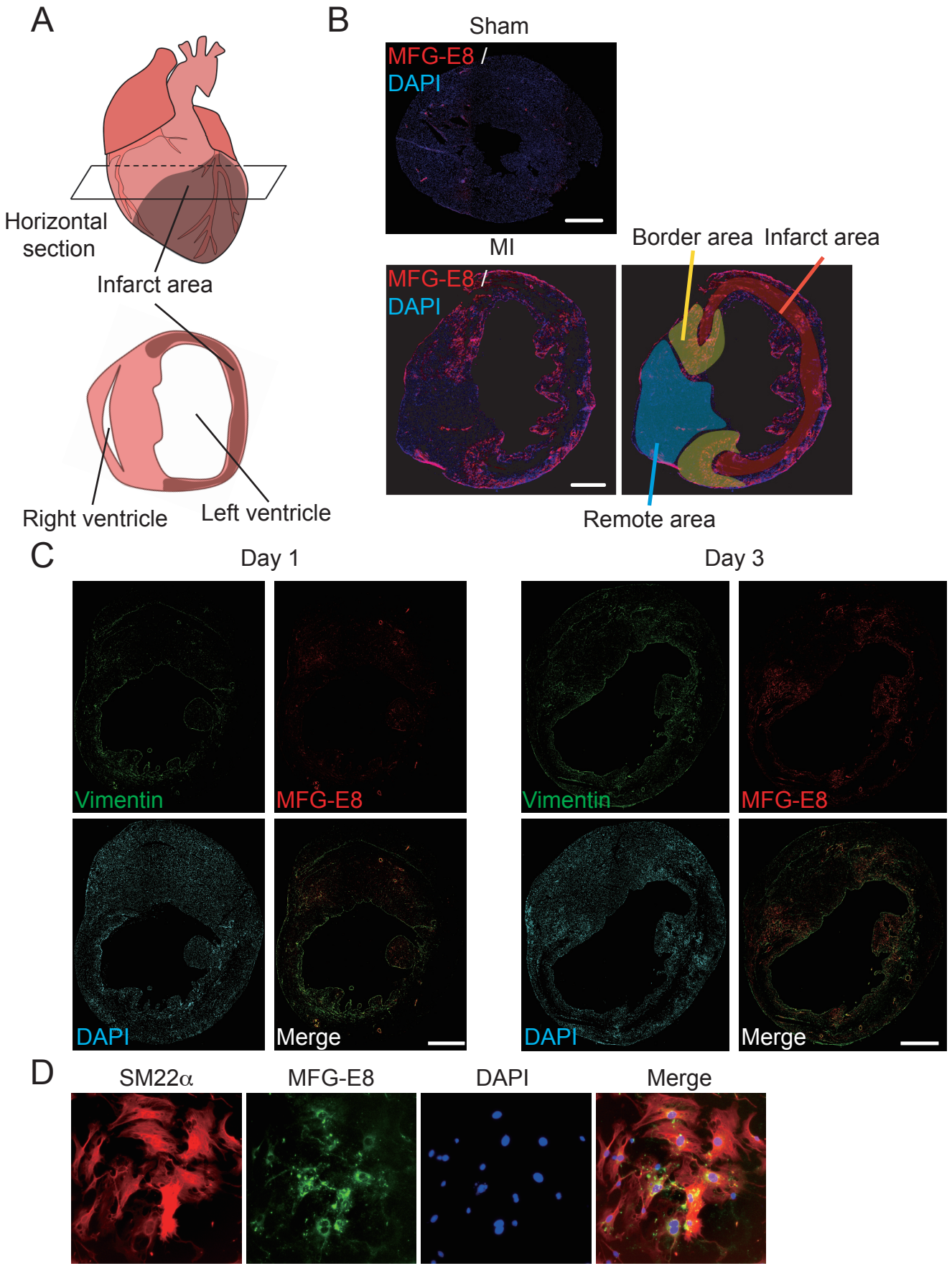

Supplemental Figure 7. MFG-E8 expression pattern in horizontal heart sections of mice at day 1 or 3 after MI and in the isolated cardiac myofibroblasts.

(A) Schematic representation of the position of mouse horizontal heart sections used for the study. (B) Representative heart sections of sham-operated or infarcted mice were stained with anti-MFG-E8 antibody (n = 4). The cell nuclei were stained with DAPI. Definitions of the "Infarct area," "Border area," and "Remote area" in infarcted hearts were shown in the right panel. Scale bar, 1 mm. (C) Localization of vimentin (green) and MFG-E8 (red) immunoreactivities in the infarcted heart at 1 day and 3 days after operation (n = 4). The cell nuclei were stained with DAPI. The image at the lower right represents two-color (anti-vimentin and anti-MFG-E8) overlay image. Representative images were shown. Scale bar, 1 mm. (D) Representative images of myofibroblasts co-expressing SM22α and MFG-E8. Isolated cardiac myofibroblasts cultured on 8-well chamber slides were stained with antibodies against SM22α and MFG-E8 (n = 4). Nuclei were labeled with DAPI. Scale bar, 100 μm.

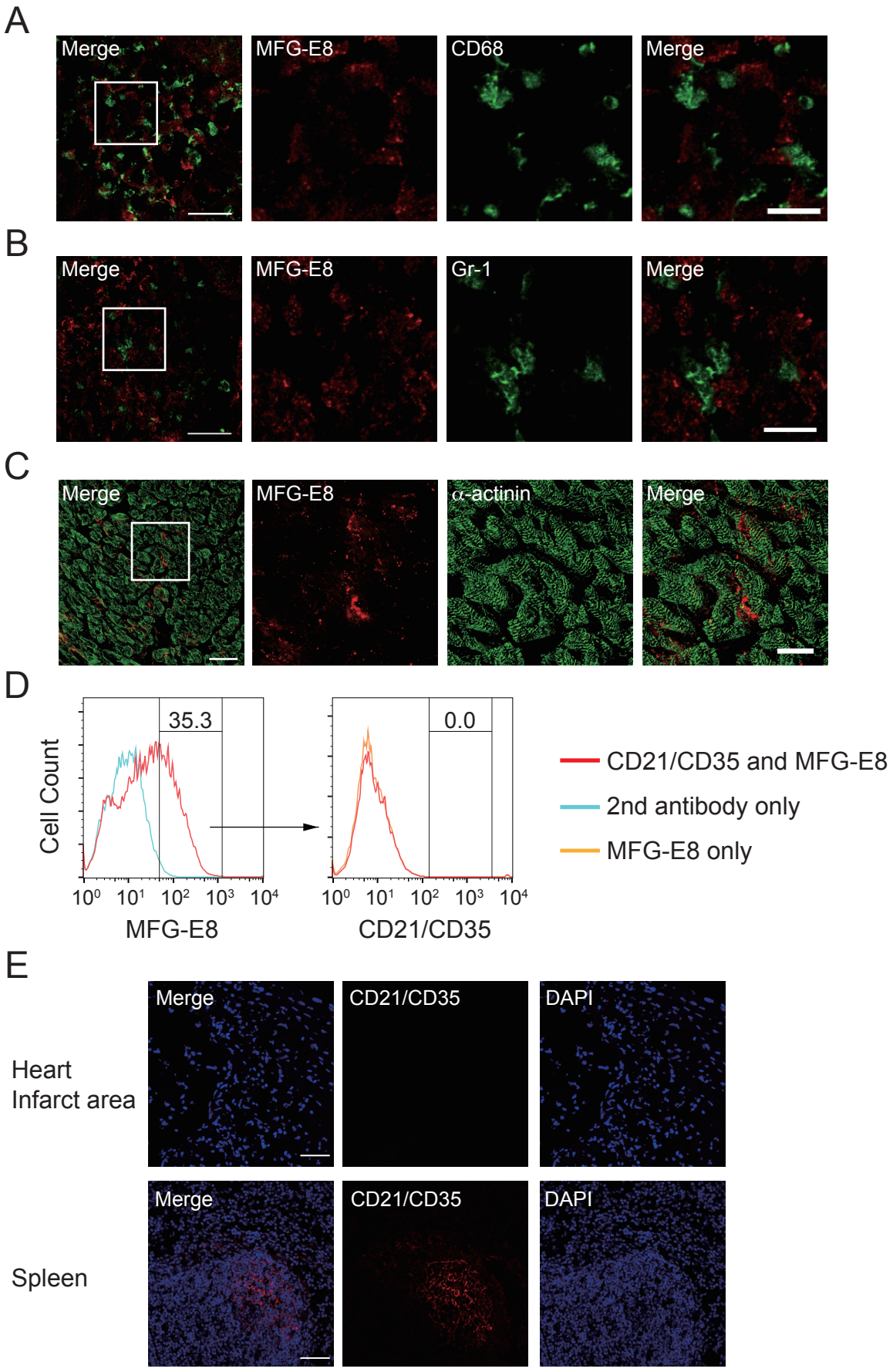

Supplemental Figure 8. MFG-E8 is not expressed in cardiomyocytes, macrophages, neutrophils or follicular dendritic cells in the infarcted left ventricles of WT mice 3 days after MI.
(A-C) The heart sections from WT mice 3 days after MI were stained with antibodies against MFG-E8 and CD68 (A), Gr-1 (B), or α-actinin (C) (*n* = 4). White squares on the merged images (first columns) mark the areas shown at a higher magnification. Higher-magnification images were shown on the right side of lower-magnification images. Scale bar, 50 μm (lower magnification), 20 μm (higher magnification). (D) Cardiac myofibroblasts isolated from WT mice on 3 days after MI were stained with anti-MFG-E8 and PE-anti-CD21/CD35 antibodies and analyzed by flow cytometry (*n* = 4). (E) Heart sections from WT mice on 3 days after MI (upper panels) and spleen sections from intact WT mice (lower panels) were stained with anti-CD21/CD35 antibody (red) and DAPI (blue). Scale bar, 50 μm.

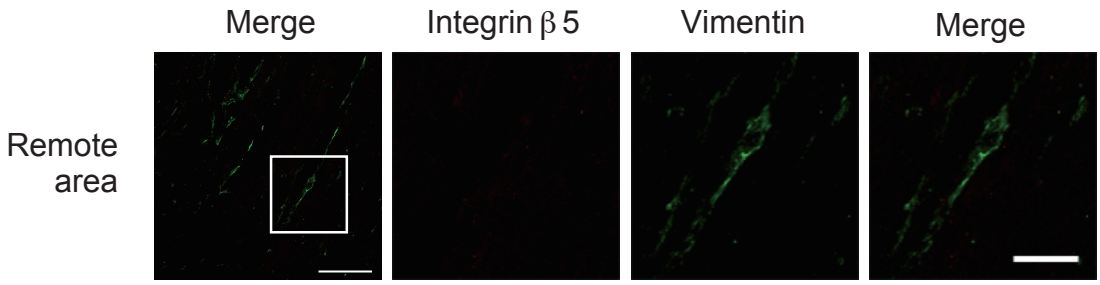

Supplemental Figure 9. Integrin β5 was not expressed in remote areas of infarcted hearts. Representative images of integrin β5 (red) and vimentin (green) staining of remote area of heart sections from WT mice 3 days after MI (*n* = 3). A square on the first column marks the area shown at a higher magnification. Scale bar, 50 μm (lower magnification), 20 μm (higher magnification).

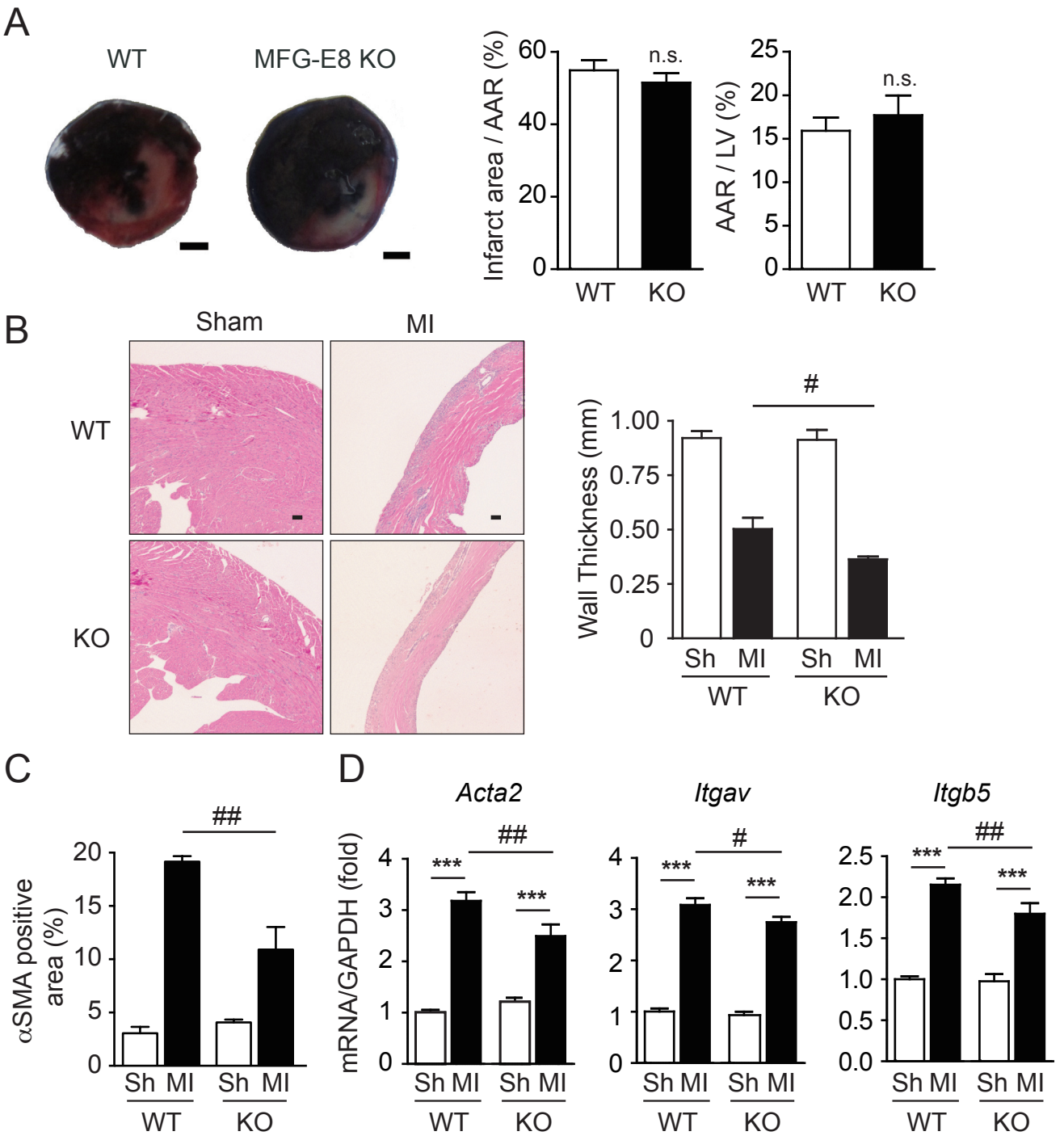

Supplemental Figure 10. Deficiency of MFG-E8 leads to thinner left ventricular walls at day 3 after MI and decreased the number of cardiac myofibroblasts in the infarcted hearts.

(A) Representative images of Evans blue/TTC staining of hearts at 3 hours after MI. Scale bar, 1 mm. Infarct size and the area at risk (AAR) were quantified as a percentage of the AAR and left ventricular area of the section, respectively (WT, *n* = 5; KO, *n* = 4), and they are shown in the graphs. (B) H&E staining of the cardiac sections of WT and MFG-E8 KO mice at day 3 after sham (Sh) or MI operation. Representative images focused on left ventricular free walls are shown. Wall thickness was determined by measuring the thickness of the left ventricular wall at three points for each group (*n* = 5−6, each group). Scale bar, 100 μm. (C) Heart sections of WT and MFG-E8 KO mice at day 3 after MI was stained by αSMA antibody. The bar graph shows the areas occupied by αSMA-positive cells (*n* = 5−6, each group). (D) mRNA expression of myofibroblast marker (*Acta2*) and integrin receptor (*Itgav*, *Itgb5*) in the hearts at 3 days after sham or MI operation of WT or MFG-E8 KO mice (WT-sh *n* = 4; WT-MI *n* = 7; KO-sh; *n* = 4, KO-MI; *n* = 5). Error bars represent the mean ± SEM. Comparisons between two groups or among groups were assessed with unpaired two tailed Student's *t* test or one-way ANOVA followed by Newman-Keuls analysis, respectively. *** $P < 0.001$, # $P < 0.05$, ## $P < 0.01$, n.s., not significant.

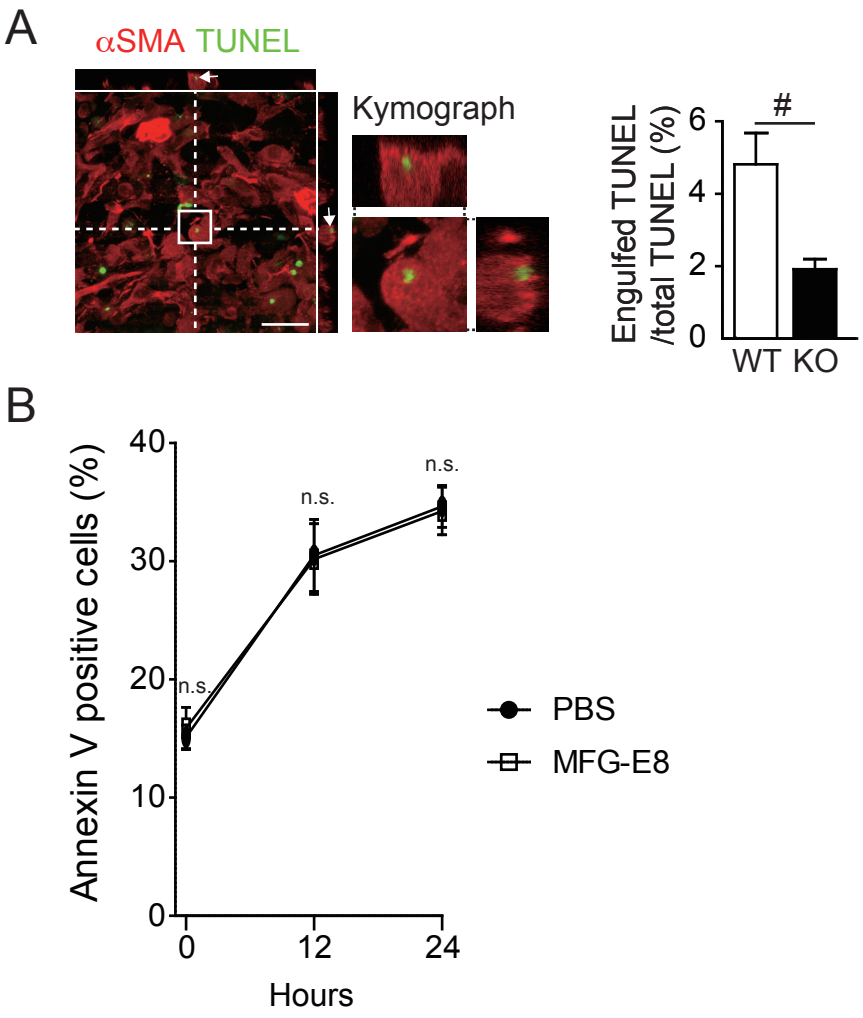

Supplemental Figure 11. MFG-E8 promotes the engulfment of apoptotic cells by myofibroblasts and did not influence the apoptosis of cardiomyocytes.
(A) Cardiac sections of WT mice at day 3 after MI were stained with αSMA (red), and then apoptotic nuclei were stained with TUNEL (green). Kymographs along the white dashed line in the merged image were shown in the upper and right side of the image. The area indicated by a white square on the merged image was enlarged. Arrows indicate a myofibroblast containing an apoptotic cell. Engulfed TUNEL$^+$ apoptotic cells on the cardiac sections from WT and MFG-E8 KO mice at 3 days after MI were quantified (n = 5 each). The percentage indicates the ratio of the number of engulfed apoptotic nuclei to the total number of apoptotic nuclei. Scale bar, 20 μm. (B) Rat neonatal cardiomyocytes were incubated with 1 μM of staurosporine for the indicated periods of time after pretreatment of mouse MFG-E8 (3.2 μg/mL) (square, n = 10) or PBS (circle, n = 10) for 30 min. The apoptotic cells were quantified by flow cytometry using FITC-conjugated Annexin V. Error bars represent the mean ± SEM. Comparisons between individual groups were conducted by unpaired two tailed Student's t test. # $P < 0.05$. n.s., not significant.

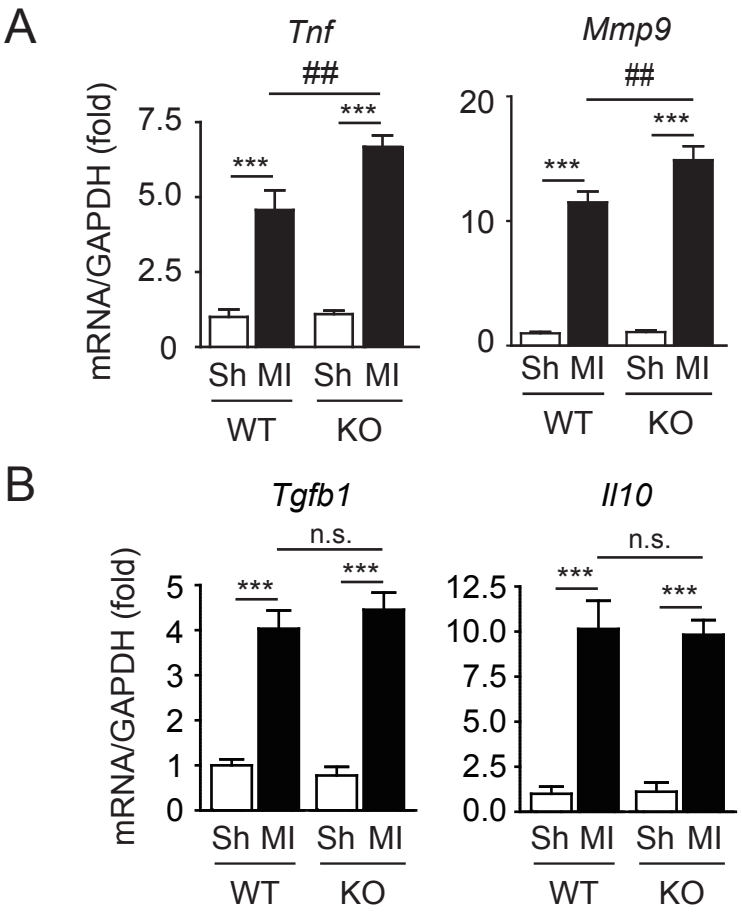

Supplmental Figure 12. MFG-E8 deficiency exacerbates inflammation at hearts after MI.
mRNA expression of pro-inflammatory genes (*Tnf and Mmp9*) (A), and anti-inflammatory genes (*Tgfb* and *Il10*) (B) in the hearts at 3 days after sham (Sh) or MI operation of WT or MFG-E8 KO mice (WT-Sh, $n = 4$; WT-MI, $n = 7$; KO-Sh, $n = 4$; KO-MI, $n = 5$). Error bars represent the mean ± SEM. Comparisons among groups were assessed with one-way ANOVA followed by Newman-Keuls analysis. *** $P < 0.001$, ## $P < 0.01$, n.s., not significant.

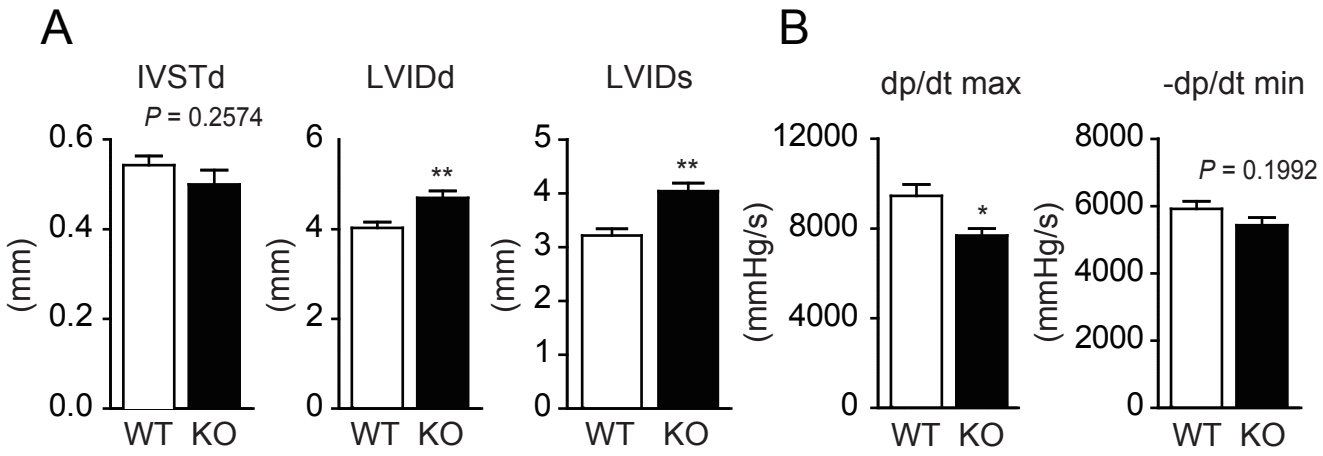

Supplemental Figure 13. MFG-E8 deficiency exacerbates cardiac function after MI.
(A) Echocardiographic measurements of WT mice (*n* = 7) or MFG-E8 KO mice (*n* = 5) at 4 weeks after MI. Interventricular septal thickness at end-diastole (IVSTd), left ventricular end-diastolic internal diameter (LVIDd), and left ventricular end-systolic internal diameter (LVIDs) are shown. (B) Hemodynamic parameters (dP/dtmax or dP/dtmin) of the WT mice (*n* = 7) or MFG-E8 KO mice (*n* = 4) at 4 weeks after MI. The parameters dP/dtmax or dP/dtmin represents the maximal rate of pressure development and minimum rate of decay of pressure, respectively. Error bars represent the mean ± SEM. Comparisons between two groups were assessed with unpaired two tailed Student's *t* test. * $P < 0.05$, ** $P < 0.01$.

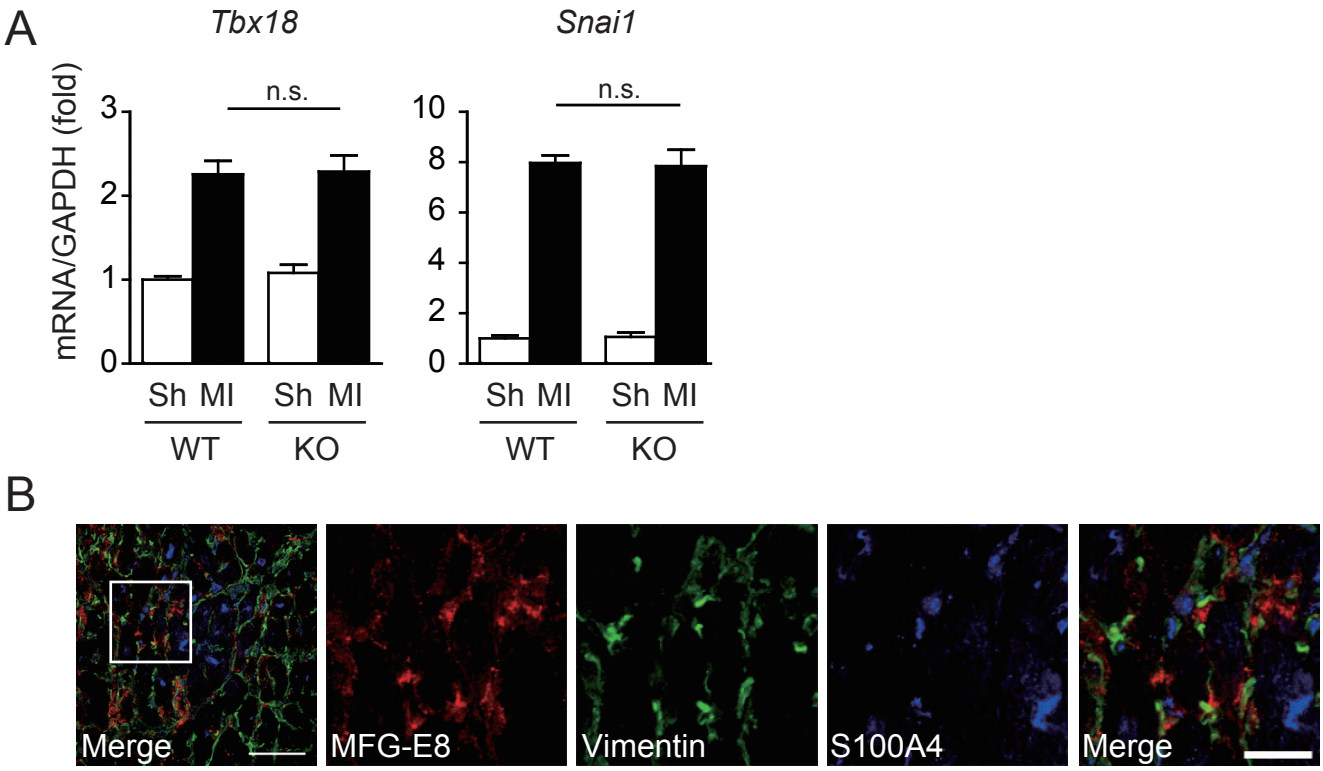

Supplemental Figure 14. MFG-E8 does not influence the expression EMT-related genes in the hearts at 3 days after MI and MFG-E8–expressing myofibroblasts did not originate from S100A4 in the infarcted left ventricles of WT mice 3 days after MI.

(A) mRNA expression of genes involved in the EndMT and EMT after sham (Sh) or MI operation in the hearts of WT or MFG-E8 KO mice. Error bars represent the mean ± SEM. Comparisons among groups were assessed with one-way ANOVA followed by Newman-Keuls analysis. n.s.; not significant (B) Left ventricular sections from WT mice on day 3 after MI were stained with anti-MFG-E8 (red), anti-vimentin (green), and anti-S100A4 (blue) antibodies. A white square on the merged image (first column) marks the area shown at a higher magnification. Higher magnification images were shown on the right side of the lower-magnification image. Scale bar, 50 μm (lower magnification), 20 μm (higher magnification).

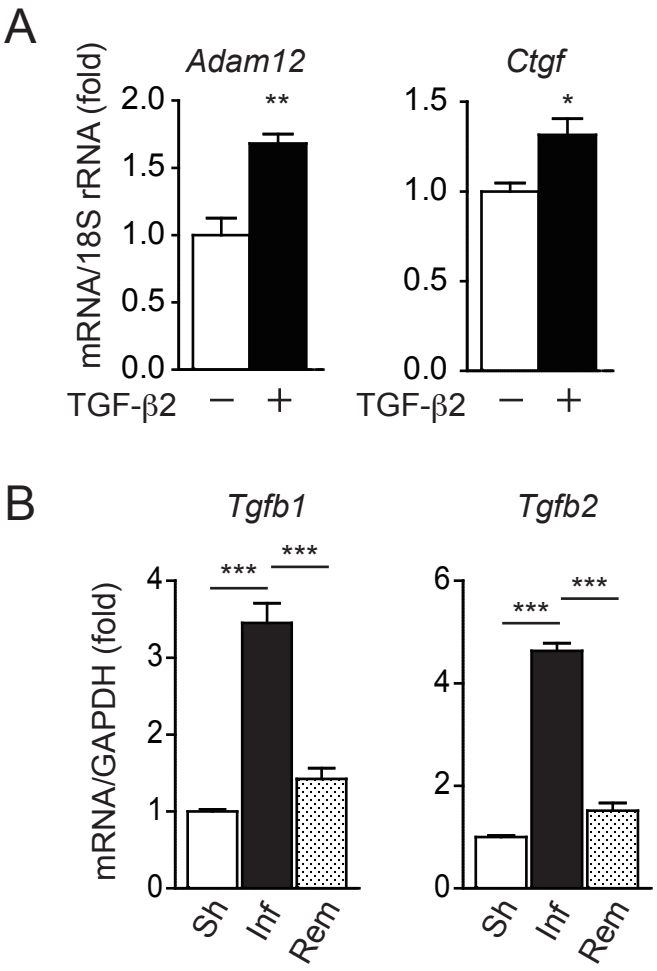

Supplemental Figure 15. Expression of fibrosis-relateged genes in HUVECs treated with TGF-β2 and expression of TGF-β1 and TGF-β2 in the infarcted area of mouse hearts 3 days after MI.

(A) *Adam12* and *Ctgf* mRNA expression levels in HUVECs treated with or without TGF-β2 (10 ng/mL) for 72 h (n = 5). Comparisons among groups were assessed with unpaired two tailed Student's *t* test. * $P < 0.05$, ** $P < 0.01$. (B) mRNA expression levels of TGF-β1 and TGF- β2 in the hearts of sham (Sh)-operated mice (white bars) (n = 3) or the infarcted (Inf) (black bars) (n = 5) or remote (Rem) areas (dotted bars) (n = 5) of the hearts of mice 3 days after MI. Comparisons among groups were assessed with one-way ANOVA followed by Newman-Keuls analysis. *** $P < 0.001$.

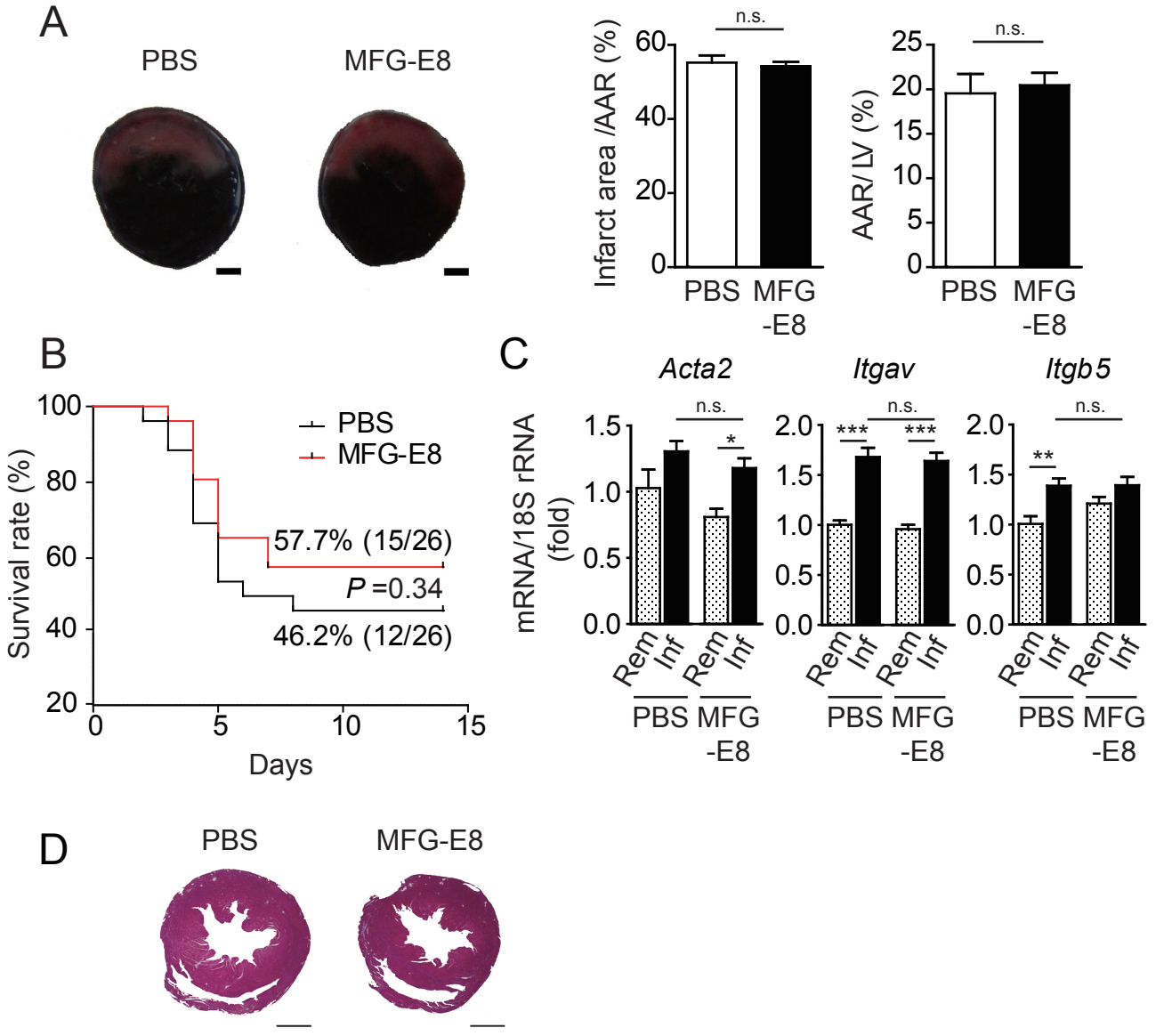

Supplemental Figure 16. Effects of MFG-E8 administration to infarcted hearts.
(A) Representative images of Evans blue/ TTC staining of hearts 3 hours after MI. Scale bar, 1 mm. Infarct size and the area at risk (AAR) were quantified as a percentage of the AAR and left ventricular area of the section, respectively (n = 3), and they are shown as graphs. (B) Survival curves of PBS- or MFG-E8-injected mice after MI. PBS (n = 26) or MFG-E8 (3.2 μg) (n = 26) was intramyocardially injected into the infarct region at the time of ligation of coronary artery. Kaplan-Meier survival analysis using a log-rank test. (C) *Acta2*, *Itgav* and *Itgb5* mRNA expression levels in remote (Rem) or infarcted (Inf) areas of hearts from WT mice at 3 days after MI and intramyocardial injection of PBS or MFG-E8 (3.2μg) (n = 4 each). (D) Representative Masson's trichrome-stained heart sections of PBS- (n = 4) or MFG-E8–administered mice (n = 4) at 10 weeks after sham-operation. Scale bar, 1 mm. Error bars represent the mean ± SEM. Comparisons between two groups or among groups were assessed with unpaired two tailed Student's t test or one-way ANOVA followed by Newman-Keuls analysis, respectively. * $P < 0.05$, ** $P < 0.01$, *** $P < 0.001$, n.s., not significant.

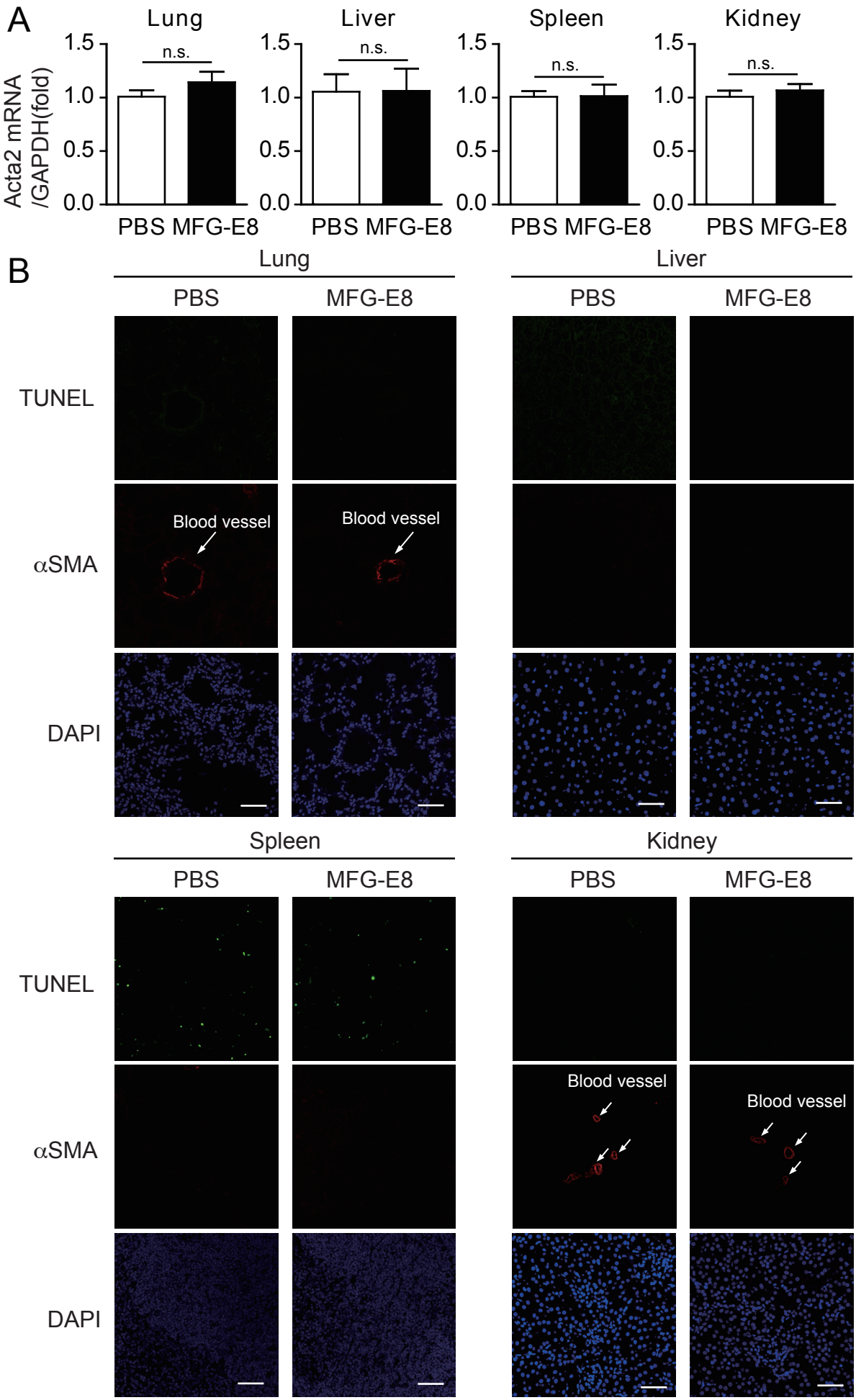

Supplemental Figure 17. Intramyocardial injection of MFG-E8 does not affect mobilization of myofibroblast and apoptotic clearance in tissues other than heart.

(A) *Acta2* mRNA levels in the lungs, livers, spleens and kidneys from WT mice on 3 days after MI and intramyocardial injection of PBS or MFG-E8 (3.2 μg) (n = 6 each). (B) Representative images of lung, liver, spleen and kidney sections from WT mice at 3 days after MI and intramyocardial injection of PBS or MFG-E8 (3.2 μg) were stained with TUNEL (green) and anti-αSMA antibody (red) (n = 6 each). Scale bar; 50 μm. Error bars represent the mean ± SEM. Comparisons among groups were assessed with unpaired two tailed Student's t test. n.s., not significant.

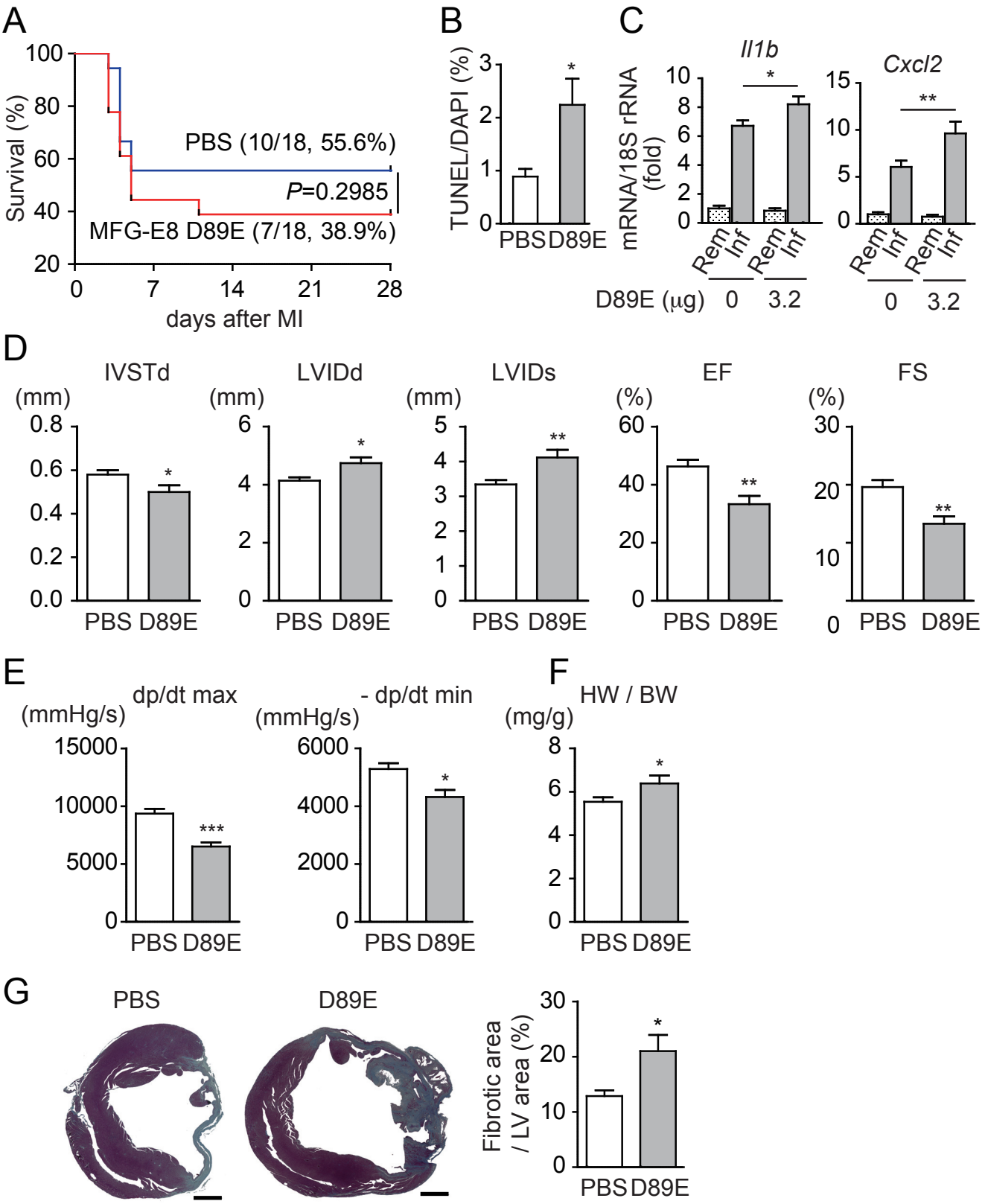

Supplemental Figure 18. Administration of MFG-E8 D89E after MI exacerbates cardiac function *in vivo*.
(A) Survival curves of mice subjected to the intracardiac administration of PBS (blue; *n* = 18) or MFG-E8 D89E (red; *n* = 18) after MI. Kaplan-Meier survival analysis using a log-rank test. (B) TUNEL-positive nuclei in border zone of PBS- or MFG-E8 D89E-administered mice (3.2 μg) (*n* = 8 each) 3 days after MI. (C) MFG-E8 D89E intramyocardial injection enhanced the upregulation of inflammatory genes in hearts 3 days after MI (0 μg: *n* = 8, 3.2 μg: *n* = 7). (D) Echocardiographic measurements of mice subjected to the intracardiac administration of PBS (*n* = 10) or MFG-E8 D89E (*n* = 7) at 4 weeks after MI. Interventricular septal thickness at end-diastole (IVSTd), left ventricular end-diastolic internal diameter (LVIDd), left ventricular end-systolic internal diameter (LVIDs), ejection fraction (EF), and fractional shortening (FS) are shown. (E) Hemodynamic parameters (dP/dtmax or dP/dtmin) of the PBS- (*n* = 10) or MFG-E8 D89E–treated mice (*n* = 5) at 4 weeks after MI. The parameters dP/dtmax or dP/dtmin represents the maximal rate of pressure development and minimum rate of decay of pressure, respectively. (F) Ratio of heart weight (HW) to body weight (BW) of PBS- (*n* = 10) or MFG-E8 D89E-treated mice (*n* = 7) at 4 weeks after MI. (G) Representative heart sections of PBS- or MFG-E8 D89E-administered mice (*n* = 6 in each group) at 4 weeks after MI stained with Masson's trichrome. The ratio of the fibrotic area to the left ventricular area was quantitatively estimated and shown in the graph. Scale bar, 1 mm. Error bars represent the mean ± SEM. Comparisons between two groups were assessed with unpaired two tailed Student's *t* test. * $P < 0.05$, ** $P < 0.01$, *** $P < 0.001$, n.s., not significant.

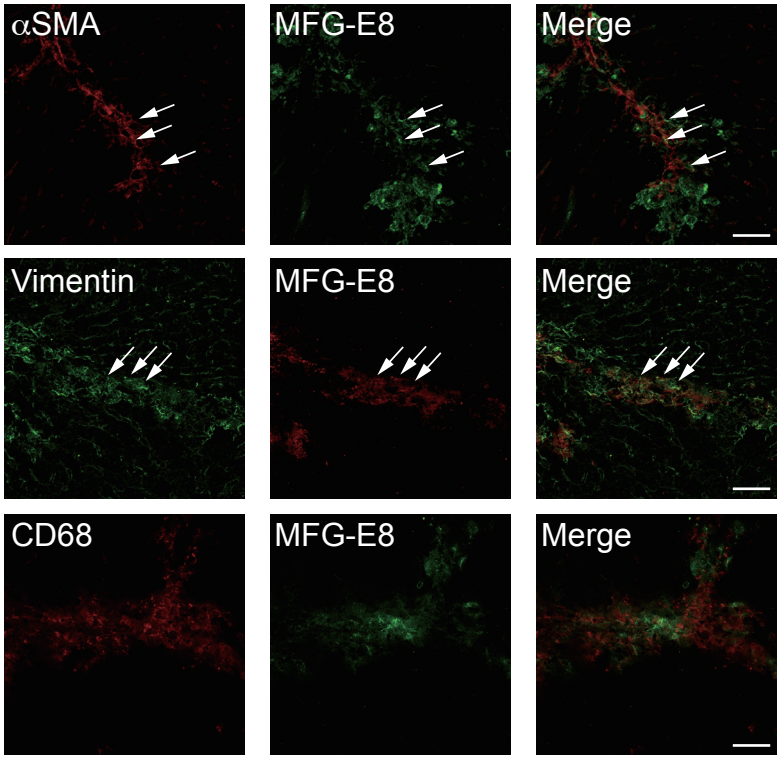

Supplemental Figure 19. MFG-E8 expression in the liver after the intraperitoneal injection of CCl_4.
WT mice were injected intraperitoneally with CCl_4 (1 ml/kg body weight, 1:4 dilution in corn oil) twice a week for 4 weeks. Liver sections from the CCl_4-treated mice were immunostained with antibodies for MFG-E8 and αSMA (upper panel), vimentin (middle panel) or CD68 (lower panel). Arrows indicate merged cells. Scale bar, 50 μm.

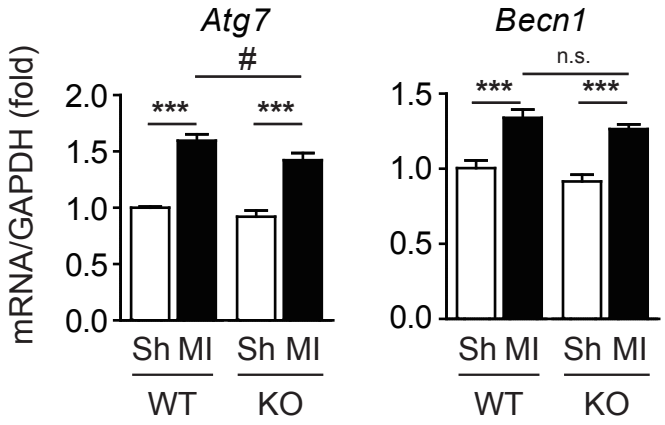

Supplemental Figure 20. Expressions of autophagy-related genes in the hearts after MI.
mRNA expression of autophagy genes (*Atg7*, *Becn1*) in the hearts on 3 days after sham- (sh) or MI-operation of WT or MFG-E8 KO mice (WT-Sh; $n = 4$, WT-MI; $n = 7$, KO-Sh; $n = 4$, KO-MI; $n = 5$). Error bars represent the mean ± SEM. Comparisons among groups were assessed with one-way ANOVA followed by Newman-Keuls analysis. *** $P < 0.001$, # $P < 0.05$, n.s. not significant.

Supplemental Table 1. Analysis of cardiac functions of WT and MFG-E8 KO mice.

	parameters	WT	KO
Organ weight	n	N = 7	N = 7
	HW/BW (mg/g)	4.738±0.089	4.588±0.135
	LW/BW (mg/g)	6.056±0.066	6.211±0.095
Echocardiography	n	N = 7	N = 7
	HR (bpm)	500±0	500±0
	LVIDd (mm)	2.057±0.053	2.157±0.037
	LVIDs (mm)	0.4857±0.063	0.6143±0.046
	%EF	98.29±0.47	97.43±0.65
	%FS	76.71±2.7	72.14±2.4
Hemodynamic analysis	n	N = 6	N = 6
	HR (bpm)	497.1±3.1	495.6±2.4
	dP/dt_{max} (mmHg/s)	11904±350	11180±522
	$-dP/dt_{min}$ (mmHg/s)	7080±300	7308±323
	EDP (mmHg)	2.839±0.700	2.598±0.612
	Tau (ms)	10.90±0.65	9.59±0.25

HW: heart weight, BW: body weight, LW: lung weight, LVIDd: LV inner diameter diastolic, LVIDs: LV inner diameter systolic, %EF: percent ejection fraction, %FS: percent fractional shortening. HR: heart rate, EDP: end-diastolic pressure, Tau: monoexponential time constant of relaxation, dP/dt max: maximal rate of pressure development, dP/dt min: minimum rate of decay of pressure.